

Effect of Cr_2O_3 Addition on the Bioactivity and Physico-Mechanical Properties of 45S5 Bioactive Glass and Glass-Ceramic

Vikash Kumar Vyas^{*}, Arepalli Sampath Kumar, Himanshu Tripathi, S.P.Singh and Ram Pyare

Department of Ceramic Engineering,
Indian Institute of Technology (Banaras Hindu University)
Varanasi, India-221005.

Abstract-- The series of chromium oxide have been partially substituted into the base bioactive glass and its effects on bioactivity and mechanical behavior have been evaluated. On addition of Cr_2O_3 in 45S5 bioactive glass, the nucleation and crystallization temperatures were found to decrease which was confirmed by Differential Thermal Analysis (DTA). The controlled heat treatment was carried out to convert bio-glass in to glass-ceramics. The developed crystalline phase was identified by X-ray diffraction (XRD) technique. The bioactivity of the prepared samples was evaluated after soaking in simulated body fluid (SBF) for various time periods. The formation of hydroxy apatite was identified by pH measurement, FTIR Spectroscopy, X-ray diffraction and Scanning Electron Microscopic (SEM) techniques. The densities of prepared bio-glass and glass-ceramics densities were found to increase. Flexural strength was also measured and found to increase with an increase in the concentration of chromium oxide in the base glass.

Key words: Bioactive glass, Transition Metal oxide (Cr_2O_3), FTIR-Spectroscopy, X-ray diffraction, Bioglass-ceramic, Mechanical properties and SEM.

I. INTRODUCTION

Generally, the purpose of biomaterials is to substitute for damaged or diseased bone tissues. Biomaterials with the property of bioactive materials were considered to be the first generation materials applied mainly at the host tissue so as to reduce the development of any inflammation or wound. Bio-glass developed by Hench, was to provide a controlled release of calcium and sodium ions under physiological condition [1]. These ions then precipitated into amorphous calcium phosphate which later crystallize

into hydroxyapatite to form new bone material(8-10). In addition to provide the fundamental building block of bone(HCA) the dissolution products of bioglasses were also found to stimulate osteoblast activity [2,3]. More recently bioactive glasses have been developed to provide a controlled release mechanism for antimicrobial ions such as Ag and Ga to combat infections[4,5]. The key compositional features that are responsible for the bioactivity of 45S5 bioactive glass are its low SiO_2 (network former) content, high Na_2O and CaO (glass network modifiers) content, and high $\text{CaO}/\text{P}_2\text{O}_5$ ratio [6]. Although 45S5 bioactive glass is biocompatible and it shows high bioactivity which is in fact clinically used for middle ear prostheses and as endosseous ridge implants [7] but, it has several limitations. A major disadvantage of 45S5 bioactive glass is connected to its fast degradation rate. In addition, the mechanical properties of 45S5 bioactive glass are not completely adequate for significant load-bearing applications [8]. Lot of researches have been carried out for preparation and characterization of bioglasses and glass-ceramics, incorporated with some ions such as Ti, K, Zr, Li, Fe, Zn, Mg and Sr because of their unique effect on osteoblastic cell proliferation, differentiation and thus bone mineralization [9-14].

The aim of substitution of chromium oxide in place of silica in 45S5 system is to investigate the effect of chromium ions on the, physicochemical properties, bioactivity, mechanical properties and glass composition.

Table 1: Composition of bioactive glasses (wt %)

| | SiO ₂ | Na ₂ O | CaO | P ₂ O ₅ | Cr ₂ O ₃ |
|------------|------------------|-------------------|-------|-------------------------------|--------------------------------|
| 45S5(Base) | 45.00 | 24.50 | 24.50 | 6.00 | 0.00 |
| Cr1 | 44.50 | 24.50 | 24.50 | 6.00 | 0.50 |
| Cr2 | 44.00 | 24.50 | 24.50 | 6.00 | 1.00 |
| Cr3 | 43.50 | 24.50 | 24.50 | 6.00 | 1.50 |
| Cr4 | 43.00 | 24.50 | 24.50 | 6.00 | 2.00 |

Table 2:-Ion concentration (mM) of simulated body fluid and human blood plasma

| Ion | Na ⁺ | K ⁺ | Mg ⁺ | Ca ₂ ⁺ | HCO ₃ ⁻ | HPO ₄ ⁻ | SO ₄ ²⁻ | Cl ⁻ |
|----------------------|-----------------|----------------|-----------------|------------------------------|-------------------------------|-------------------------------|-------------------------------|-----------------|
| Simulated body fluid | 142.0 | 5.0 | 1.5 | 2.5 | 4.2 | 1.0 | 0.5 | 147.8 |
| Human blood plasma | 140.0 | 5.0 | 1.5 | 2.5 | 27.0 | 1.0 | 0.5 | 103.0 |

Table.3 Heat treatment temperatures used for nucleation and crystal growth of bioglasses

| Sample | First nucleation temperature (°C) | Soaking time (hrs) | Crystallization temperature (°C) | Soaking time (hrs) |
|--------|-----------------------------------|--------------------|----------------------------------|--------------------|
| Cr 0 | 609 | 6 | 755 | 3 |
| Cr1 | 586 | 6 | 721 | 3 |
| Cr2 | 581 | 6 | 712 | 3 |
| Cr3 | 553 | 6 | 690 | 3 |
| Cr4 | 547 | 6 | 676 | 3 |

Table 4:- Flexural strength and Density of bio-glasses and glass-ceramic

| Sample | Density (g/cm ³) | | Flexural strength (MPa) | |
|--------|------------------------------|---------------|-------------------------|---------------|
| | Bioglass | Glass-ceramic | Bioglass | Glass-ceramic |
| 45S5 | 2.6 | 2.81 | 44.48 | 104.27 |
| Cr1 | 2.63 | 2.84 | 54.25 | 114.47 |
| Cr2 | 2.64 | 2.87 | 61.42 | 120.21 |
| Cr3 | 2.65 | 2.88 | 70.52 | 129.32 |
| Cr4 | 2.67 | 2.89 | 77.58 | 135.95 |

Table.5 Functional group of infrared wavenumbers in a bioactive glasses surface before and after SBF treatment

| Wavenumber (cm ⁻¹) | Functional Groups |
|--------------------------------|-------------------------|
| 400 - 500 | Si-O-Si (bend) |
| 500 - 560 | P-O(Bend) (Crystalline) |
| 560 - 600 | P-O(Bend) (Amorphous) |
| 720 - 840 | Si-O-Si (Tetrahedral) |
| 860 - 940 | Si-O (Stretch) |
| 1000 - 1100 | Si-O-Si (Stretch) |
| 1100 - 1200 | P-O (Stretch) |
| 1400 - 1530 | C-O (Stretch) |
| 1600 - 1900 | C=O (Stretch) |
| 3000 - 3700 | O-H (Stretch) |

Table.6 The changes in infrared spectra of bioglasses samples peak were correlated with stages of formation of hydroxyl carbonate apatite layer on the surface

| Wave number (cm ⁻¹) | Vibration mode | Surface reaction stage | Surface reaction stage |
|---------------------------------|--|------------------------|------------------------|
| 980-850 | Si-O-Si stretching mode of nonbridging oxygen atoms | | Stages 1 and 2 |
| 850-700 | Si-O-Si symmetric stretch of nonbridging oxygen atoms between tetrahedra | | Stage 3 |
| 620-520 | P-O bending (amorphous) | | Stage 4 |
| 620-520 | P-O bending (crystalline) | | Stage 5 |
| 520-560 | P-O bending (crystalline) | | Stage 5 |

B. Preparation of the bioglasses.

II. MATERIAL AND METHODS

A. Selection of composition

The bioactive glass composition was formulated from Na₂O-CaO-SiO₂-P₂O₅ glass system. First the bioactive glass 45S5 (Hench glass), having weight % composition 45 SiO₂ - 24.5 Na₂O - 24.5 CaO - 6 P₂O₅ was prepared. Then the proposed bioglass containing chemical composition (45-X) SiO₂- 24.5 Na₂O- 24.5CaO -6 P₂O₅ (Where X=0, 0.5, 1, 1.5 and 2 of Cr₂O₃) was further prepared. In this study the CaO, Na₂O and P₂O₅ percentage was kept constant and SiO₂ was partially replaced. The compositions of bioactive glasses are given in Table 1.

The analytical reagent grade chemicals from Loba Chemie, Mumbai were used for the experiment such as quartz, sodium carbonate, calcium carbonate, and chromium oxide and ammonium dihydrogen orthophosphate as a source of SiO₂, Na₂O, CaO, Cr₂O₃ and P₂O₅ respectively.

All were introduced in the form of their respective anhydrous state. The weighed batches were mixed thoroughly for 30 minutes and melted in alumina crucibles to get the desired bioglasses as given above in table 1. The melting was carried out in an electric furnace at 1400±5°C for 2 hours in air as furnace atmosphere and homogenized melts were poured on preheated aluminum sheet. The

prepared bioglass samples were directly transferred to a regulated muffle furnace at 470°C for annealing. After 1 hour of annealing the muffle furnace was cooled to room temperature with controlled rate of cooling at 10°C per min.

C. Preparation of SBF

Kokubo and his colleagues developed simulated body fluid that has inorganic ion concentrations similar to those of human body fluid in order to reproduce formation of apatite on bioactive materials in vitro [15]. The SBF solution was prepared by dissolving reagent-grade NaCl, KCl, NaHCO₃, MgCl₂·6H₂O, CaCl₂ and KH₂PO₄ into double distilled water and it was buffered at pH=7.4 with TRIS (trishydroxymethyl aminomethane) and 1N HCl at 37 °C as compared to the human blood plasma (WBC). The ion concentrations of SBF are given in the Table 2.

D. Characterization of samples

- Differential Thermal analysis measurements (DTA)

Differential Thermal Analysis (SETARAM Instrumentation, France) was carried out on powdered bioglass samples in air up to 1000 °C using a powdered alumina as a reference material and the heating rate was 10°C min⁻¹. The glass nucleation and crystallization temperatures were obtained from the DTA results which were used for proper heat treatment for converting glass to their corresponding glass-ceramic derivatives with high crystalline. The obtained temperatures are given in Table 3 for each specific composition.

- Heat-treatment regime (conversion to glass-ceramic)

The prepared bioglass samples were heat-treated in two-step system, firstly nucleation temperature for the formation of nuclei sites and after holding for the specific time, it was then further heated to reach the second selected crystal growth temperature after holding for the specific time. The samples were left to cool inside the muffle furnace to room temperature at a cooling rate of 10°C per min. The temperatures were given in Table 3 for each bioglass system.

- Powder X-ray diffraction (XRD) measurements

In order to identify the crystalline phase present in the heat-treated bioglass samples, the glass-ceramic samples were ground to 75 microns and the fine powders were subjected to X-ray diffraction analysis (XRD). A RIGAKU-Miniflex II diffractometer adopted Cu-K α radiation ($\lambda = 1.5405\text{\AA}$) with a tube voltage of 40 kV and current of 35mA in a 2θ range between 20° and 80°. The step size and measuring speed was set to 0.02° and 1° per min respectively, was used in the present investigation. The JCPDS-International Centre for diffraction Data Cards were used as a reference.

- Structural analysis of bioglasses and glass-ceramic by FTIR Reflection spectrometry

The structure of bioglasses and glass-ceramic were measured at room in the frequency range of 2000–400 cm⁻¹ using a Fourier transform infrared spectrometer, (VARIAN scimitar 1000, USA). The fine bioglass and glass-ceramic powder samples were mixed with KBr in the ratio 1:100 and the mixtures were subjected to an evocable die at load of 10 tons/cm² to produce clear homogeneous discs. The prepared discs were immediately subjected to IR spectrometer to measure the transmittance spectra in order to avoid moisture attack.

- In vitro bioactivity study of bioglass and bioglass-ceramic

In order to investigate the formation of (calcium phosphate) apatite layer on the surface of the samples after immersion in SBF solution. The sample (1g) was immersed in 10ml of SBF solution in a small plastic container at 37 °C with pH 7.40 in an incubator at static condition for the following time period 1, 3, 7 and 15 days. After soaking, the samples were filtered, rinsed with doubly distilled water, and dried in an oven at 120 °C for 2 hours before analysis by FTIR and SEM.

- Density measurement by Archimedes principle

The densities of casted bioglasses and glass-ceramic were measured by Archimedes principle with water as the immersion fluid. The measurements were performed at room temperature. Thin copper wire was used for immersing the samples into water. The density was determined from Eq 1.

$$\text{Density} = \frac{M_a}{M_a - M_i} \times 0.988 \text{ -- Eq 1}$$

Where, M_a is the mass of glass in air and M_i is the mass of immersed glass.

- pH measurement

The pH of bioglass and glass-ceramic powders (1 g) was soaked in 10 ml of SBF solution at 37 °C for different time period and the pH was measured using Universal Bio microprocessor pH meter. The instrument was calibrated each time with standard buffer solutions of pH 4.00 and 7.00 at room temperature and pH values have been recorded during different time periods at a fixed time interval.

- Surface morphology of bioglass sample by SEM

The SEM of bioglass powders (1 g) were pressed (load of 10 MPa) into pellet form using an evocable die to produce discs of 10 mm in dia. The pellets were immersed

in SBF (10 ml) for 7 days at 37 °C. The surface morphology of samples was analyzed before and after SBF treatment using a scanning electron microscope (SEM - Inspect S50, FEI). The samples were coated with gold (Au) by sputter coating instrument before analyzing with SEM.

- Flexural strength of bioglass and glass-ceramic.

III. RESULTS AND DISCUSSION

A. Differential Thermal Analysis (DTA) of Bioactive Glasses

Table 3 shows the differential thermal analysis (DTA) of bioglasses, the results shows that the nucleation temperature reduced from 537 to 609 °C and crystallization temperature reduced from 679 to 755°C. It can be seen from the Table-3 that the addition of chromium affected on both the glass transition temperature (T_g) and crystallization temperature (T_p), the peaks were decreased with increasing chromium substitution. During heat treatment process the intermediate oxides may switch their structural role into the glass; however, apart from a slight shift of the thermo grams to lower temperatures, there is no drastic change in the thermal behavior.

The melts were casted in rectangular shape mould and the resultant bioglass and glass-ceramic samples were ground and polished for required dimension using grinding machine then samples were subjected to three point bending test. The test was performed at room temperature using Instron Universal Testing Machine (AGS 10kND, SHIMADZU) of cross-head speed of 0.5mm/min and full scale load of 2500 kg.

B. X-Ray Diffraction (XRD) patterns of ceramic derivatives of bioglasses

Figure.1 shows the XRD patterns of bioglass sample after controlled thermal treatment. The entire bioglass samples show specific crystalline as $\text{Na}_2\text{Ca}_2\text{Si}_3\text{O}_9$, the intensities of the sharp diffraction peaks match with the standard PDF#: 22-1455. The same crystalline phase has been reported in previous studies on sintered 45S5 bioactive glass [16]. The minor phase found as Calcium phosphate $\text{Ca}(\text{PO}_3)_2$ PDF#: 33-500584. It is well known that the 45S5 bioglass has the tendency to form the sodium-calcium-silicate phase as the main phase silicate crystal which was also confirmed by Hench [17].

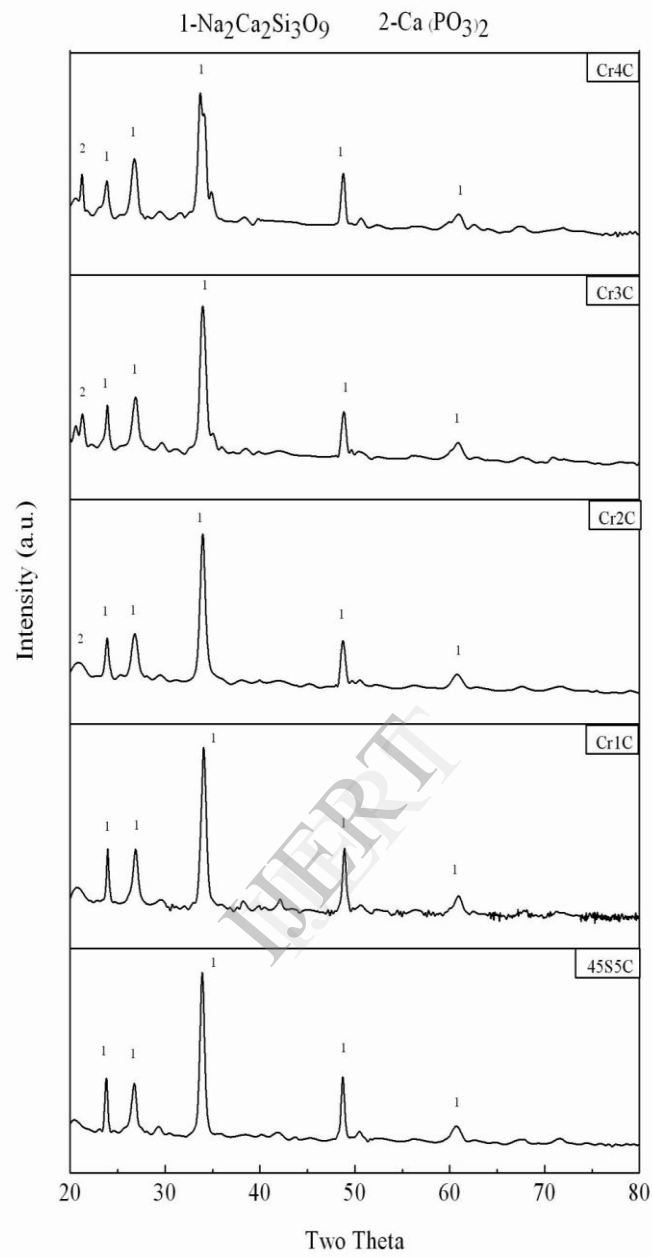


Figure1. XRD curves of bioactive glasses

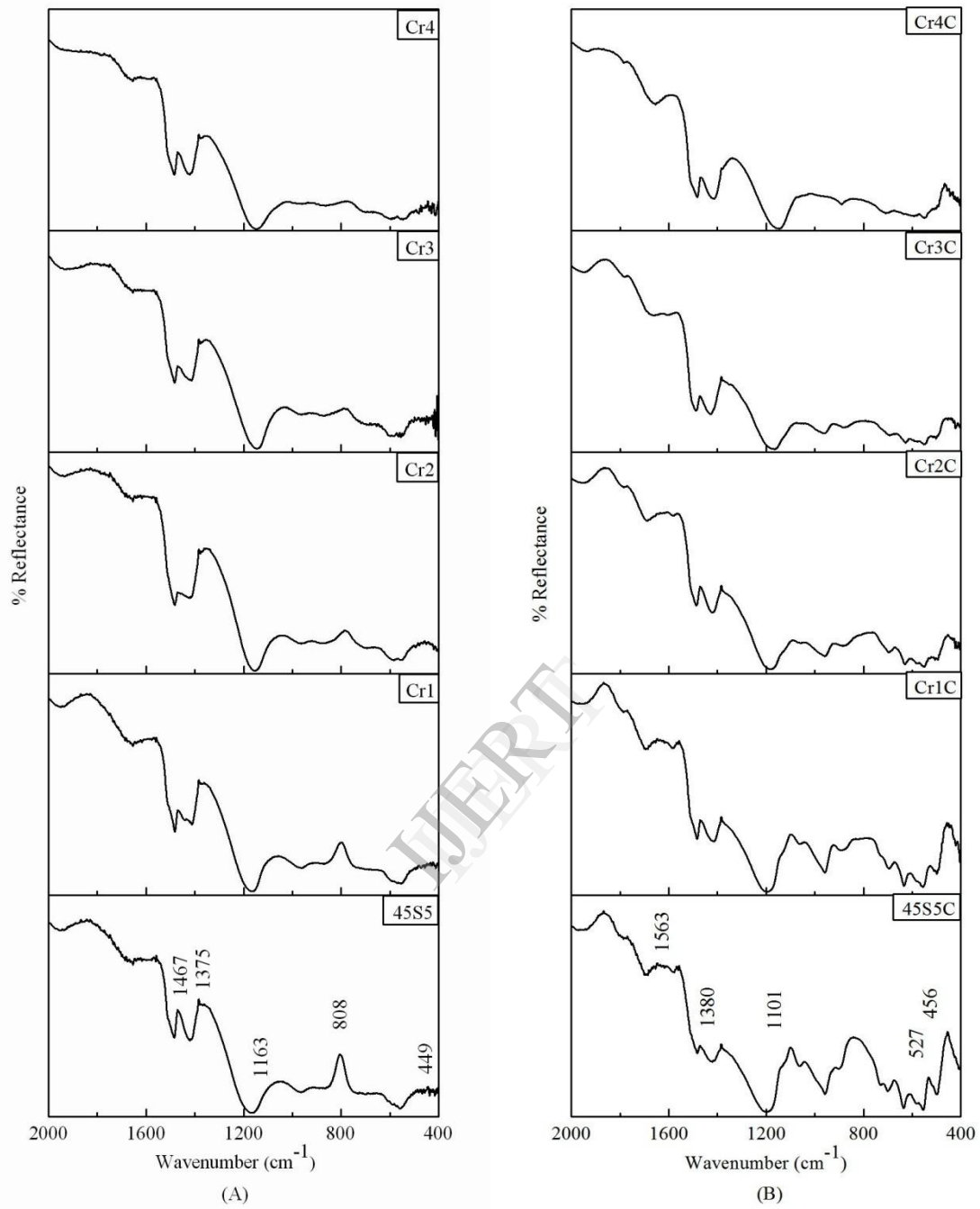


Figure 2: FTIR reflectance spectra of (A) bioactive glasses (B) bioactive glass - ceramics before immersion in SBF solution

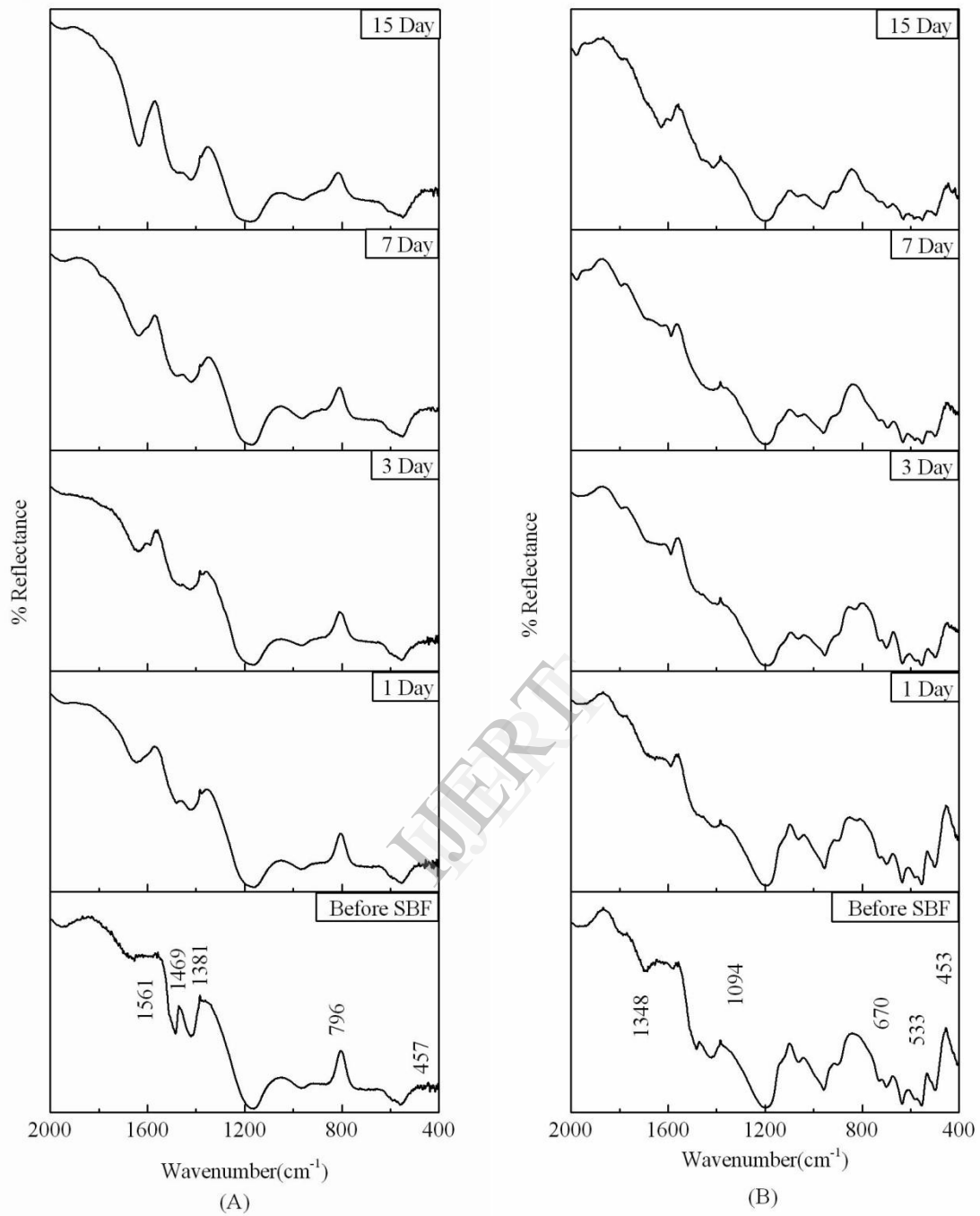


Figure 3: FTIR reflectance spectra of (A) 45S5 bioactive glasses (B) 45S5 bioactive glass - ceramics after soaking for different day in SBF solution

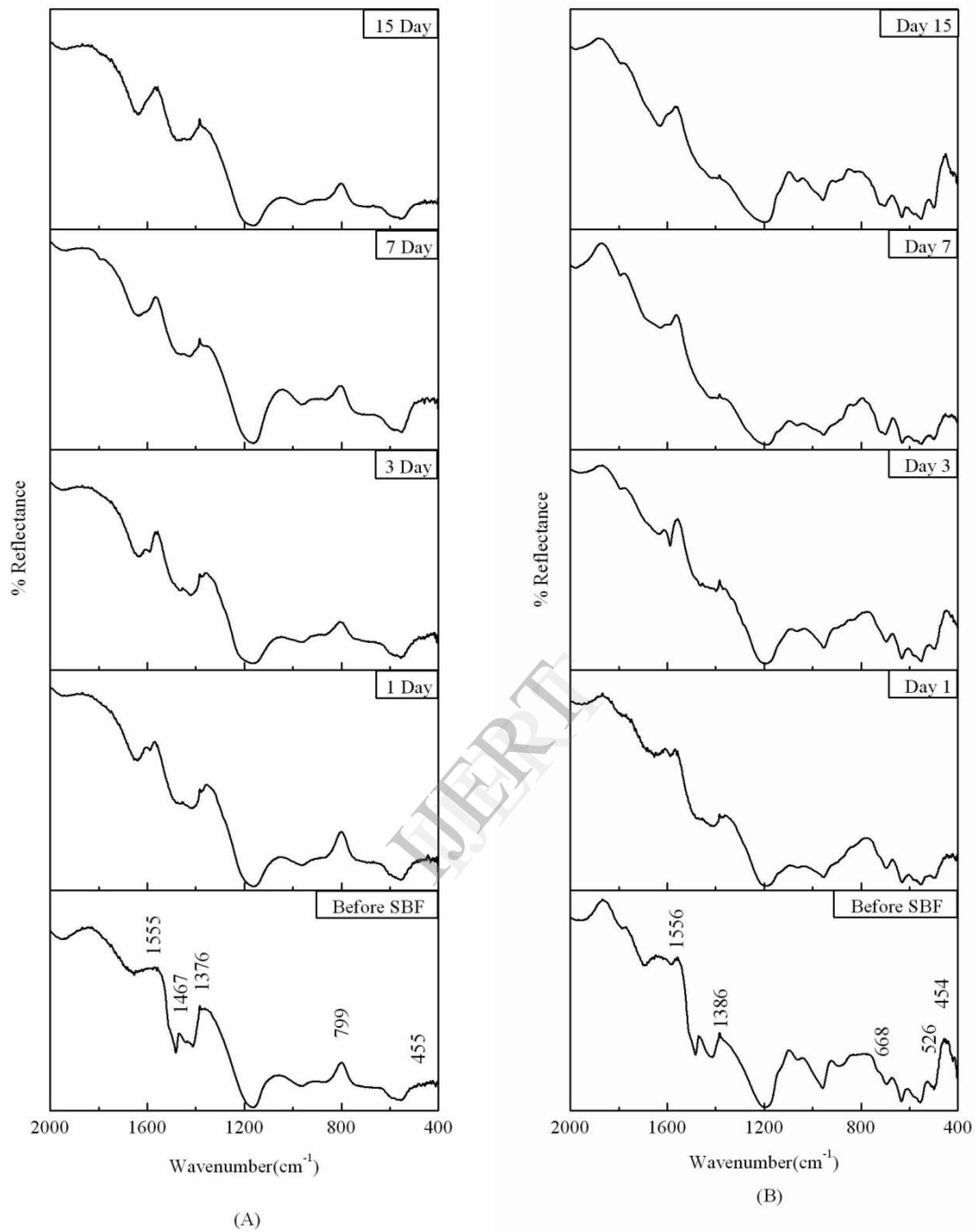


Figure 4: FTIR reflectance spectra of (A) Cr1doped bioactive glasses (B) Cr1doped bioactive glass - ceramics after soaking for different day in SBF solution

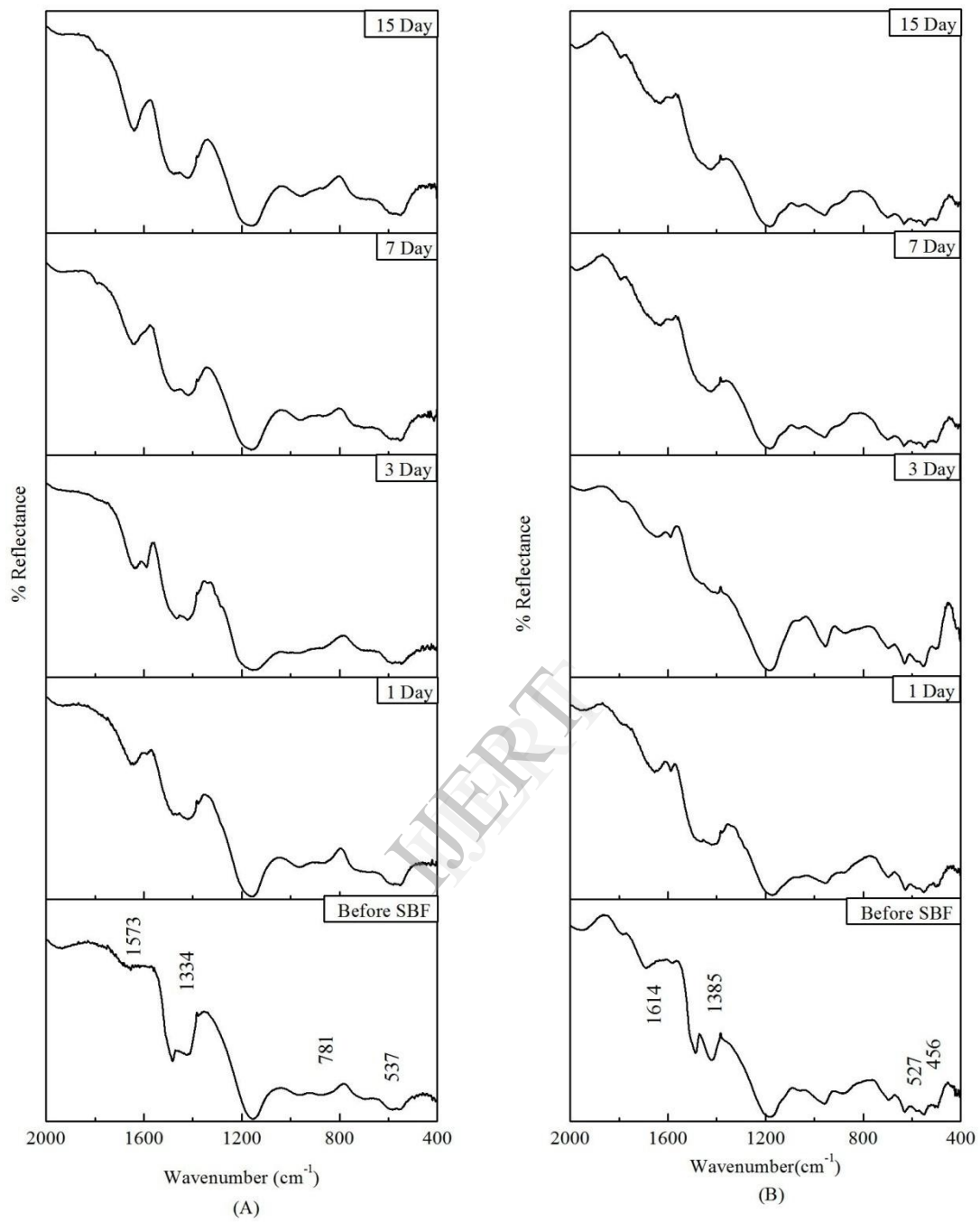


Figure 5: FTIR reflectance spectra of (A) Cr₂ doped bioactive glasses (B) Cr₂ doped bioactive glass - ceramics after soaking for different day in SBF solution

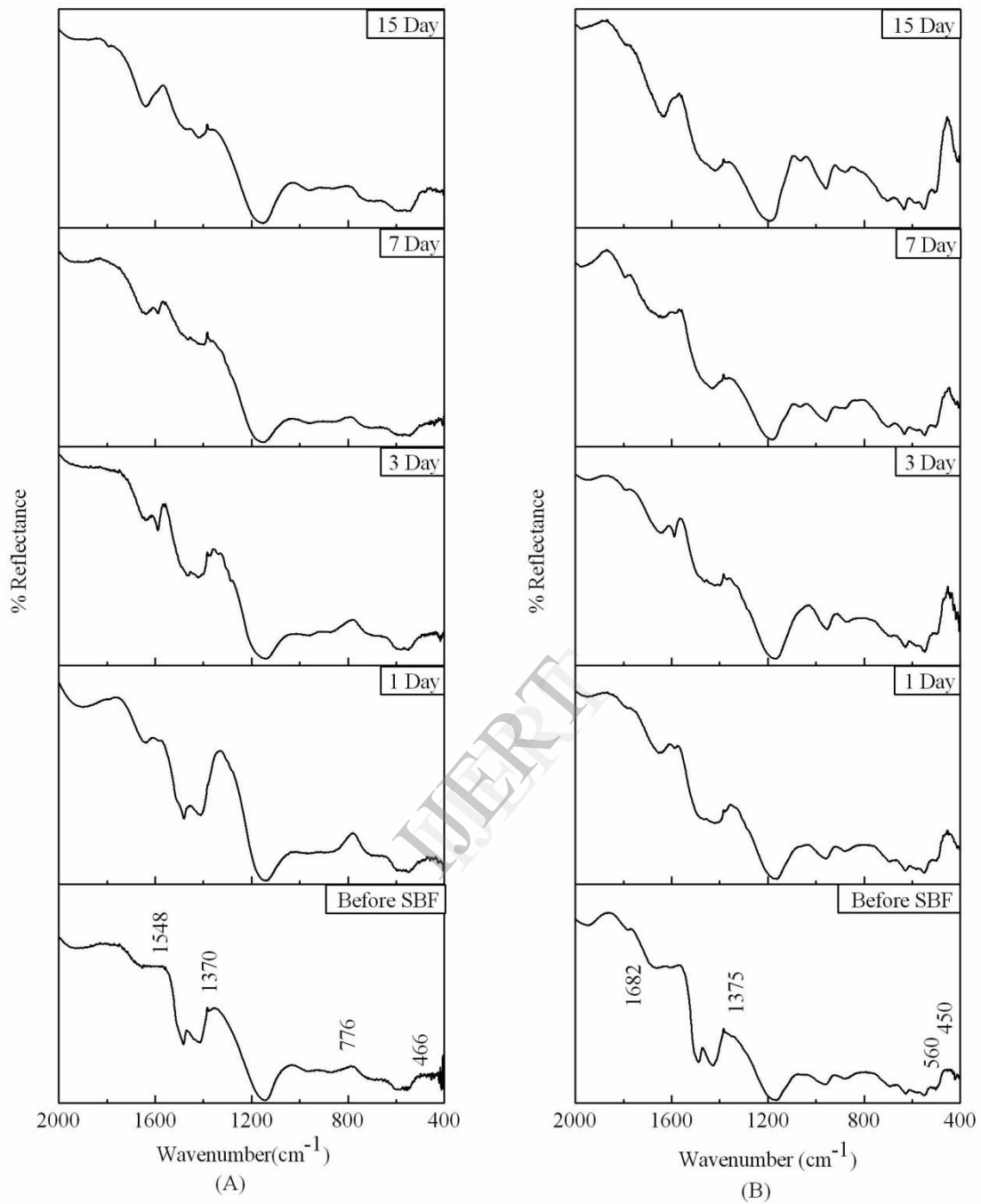


Figure 6: FTIR reflectance spectra of (A) Cr3 doped bioactive glasses (B) Cr3 doped bioactive glass - ceramics after soaking for different day in SBF solution

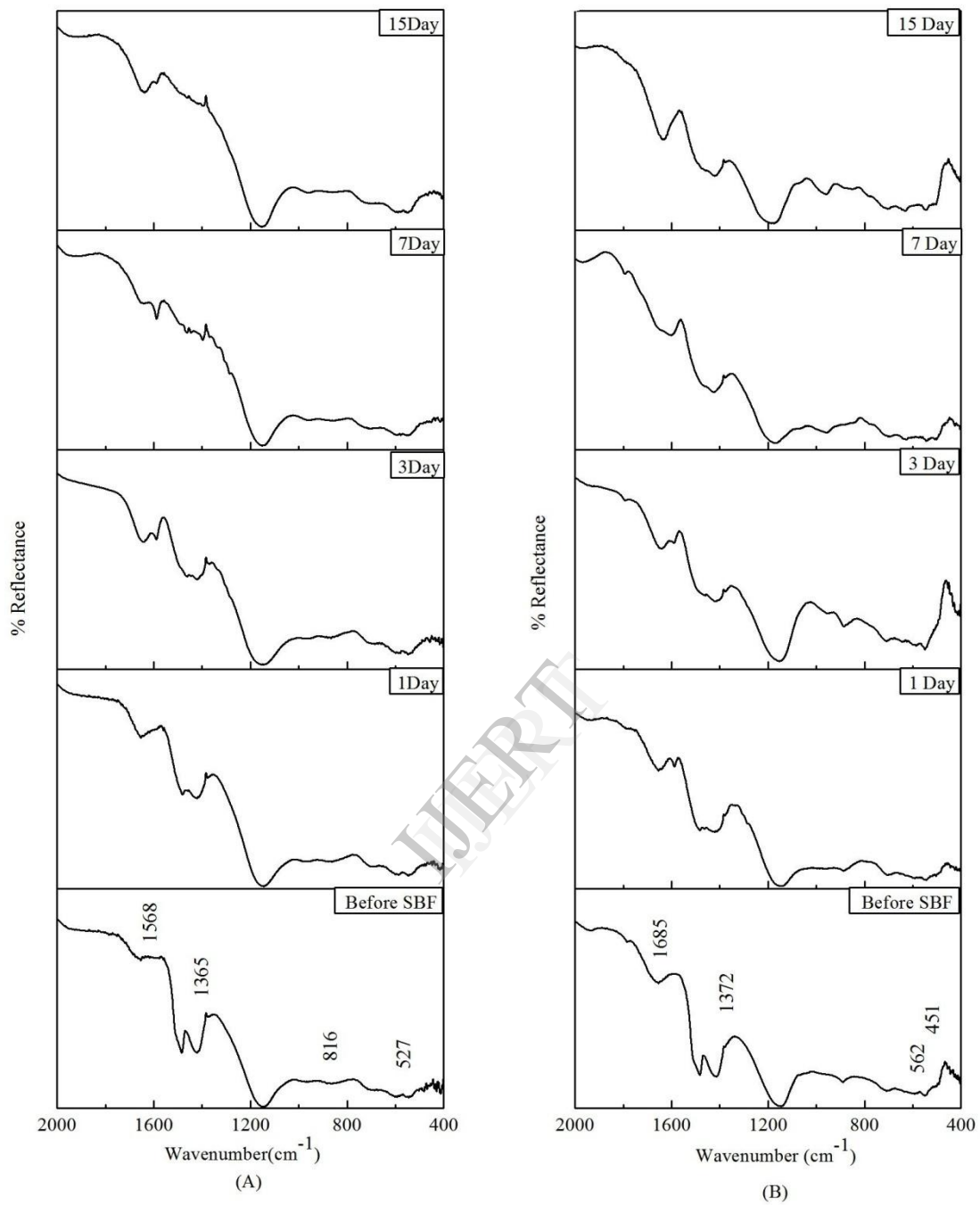


Figure 7: FTIR reflectance spectra of (A) Cr4 doped bioactive glasses (B) Cr4 doped bioactive glass - ceramics after soaking for different day in SBF solution

C. FTIR Reflection Spectra of bioglass and their ceramic derivatives

Figure 2 shows the FTIR spectra of bioglass and their ceramic derivative before SBF. In the bioglass peaks at about 449, 808, 1163, 1375 and 1467 and glass-ceramic peaks are 456, 527, 1101, 1389 and 1563 cm^{-1} . The reflection IR spectra peaks of bioglasses confirm the main characteristic of silicate network. The resultant IR spectra at 449 cm^{-1} associated with a Si-O-Si symmetric bending mode, the band at 808 cm^{-1} corresponds with Si-O-Si symmetric stretch. The major band at about 1163 cm^{-1} can be attributed to Si-O-Si stretching. The small band at 1467 cm^{-1} attributed to C-O vibrational mode. Table 5 depicts the infrared frequencies and related functional structural groups in the bioglasses [18]. In glass-ceramic 45S5 and Cr doped glass-ceramic has common peaks but 1101 cm^{-1} vanished in Cr2, Cr3 and Cr4. The P-O bending (crystalline) peak at 550-620 cm^{-1} is the characteristics peaks of calcium pyrophosphate which indicate the bioactivity of the glass ceramic. The IR spectra peaks of Cr1, Cr2, Cr3 and Cr4 samples have the same behavior of Cr0 with small change in the peaks intensities. The bioglasses substituted with chromium are not showing noticeable changes in the IR spectra bands.

D. pH behavior in SBF

The variation in pH values of simulated body fluid (SBF) solution due to soaking of bioactive glasses and glass - ceramics for various time periods is shown in Figure 8 & 9 respectively.

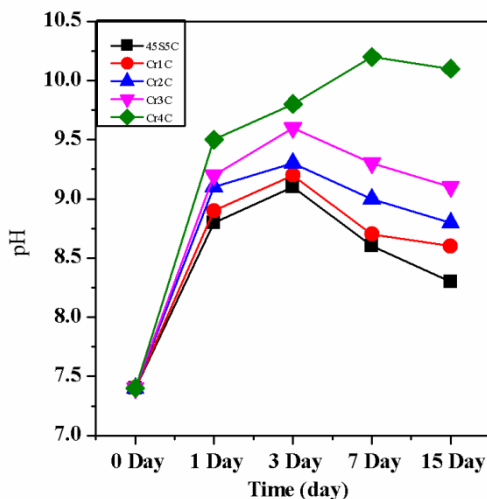


Figure.8 pH Bioglass Sample

It was observed that the addition of Cr_2O_3 in the base bioactive glass (45S5) the pH values of SBF solution increased during first 3 days of soaking due to faster release of Ca and Na ions from the sample surface caused an increase in the pH. Then it is found to decrease and attained nearly a constant value in all cases. The crystallized

bioactive glasses also showed the same behavior of decreases in pH. The reactions occurred are in favor of formation of hydroxy apatite like layer on the surface of the samples.

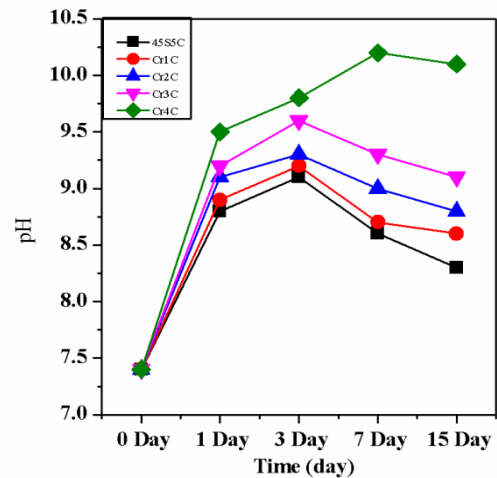


Figure.9 pH Bioglass-ceramic

E. In Vitro bioactivity of bioglasses and glass-ceramic by Reflection spectroscopy

Figures.3-7 show the FTIR Reflection spectra bands of the bioglasses and glass-ceramic before and after immersion in SBF for different time periods 0, 1, 3, 7 and 15 days.

Hench [17] studied the stages of apatite formation on the surface of the samples and spectral wavenumbers were correlated with Table 6 that the changes in the IR spectra bands after immersion in SBF for prolonged time period was also as suggested by Kim et al. [18] and Filgueira [20].

It may be seen from infrared spectra Figure 3-7 that the chromium substitutions in base bioglasses are not affected in apatite formation. Glass-ceramic before immersion in SBF solution shows the similar peaks except in glass-ceramic 1 has been extra peak at 1556 cm^{-1} one peaks in before SBF 1101 cm^{-1} vanished. After immersion in SBF solution from 1 to 15 days all sample has common peaks at around 527, 813 and 1356 cm^{-1} . The P-O stretching peak at 1000-1220 cm^{-1} indicating the formation of amorphous $\text{CaO.P}_2\text{O}_5$ rich layer. The P-O bending (crystalline) peak at 550-620 cm^{-1} is the characteristics peaks of calcium pyrophosphate which indicate the bioactivity of the glass-ceramic.

E. Surface morphology of bioglass sample by SEM

The SEM micrographs Figure 12 & 13 shows the bioglass samples (Cr0, Cr1, Cr2 and Cr3) before and after the immersion in the simulated body fluid for 7 days at 37.0 $^{\circ}\text{C}$. The micrographs exhibits the polycrystalline fine texture formed on surface layer which encourage the same

crystallinity and also comparison with the surface layer formed on the base bioglass samples [36].

F. Density of bioglasses and glass-ceramic measured by Archimedes principle

Figure 10 shows the densities of bioglasses and glass-ceramic were measured corresponding with chromium substitution (45S5-2.60, Cr1-2.63, Cr2-2.64, Cr3-2.65 and Cr4-2.67) and glass-ceramic (45S5C-2.81, Cr1C-2.84, Cr2C-2.87, Cr3C-2.88 and Cr4C-2.89). It is observed that the densities of the samples were increased with increasing chromium content from 2.60 to 2.89 gm/cm³, it may be due to partial replacement of SiO₂ with Cr₂O₃, which is attributed to the replacement of a light element (density of SiO₂ -2.63) with a heavier one (Cr₂O₃5.22) in the composition.

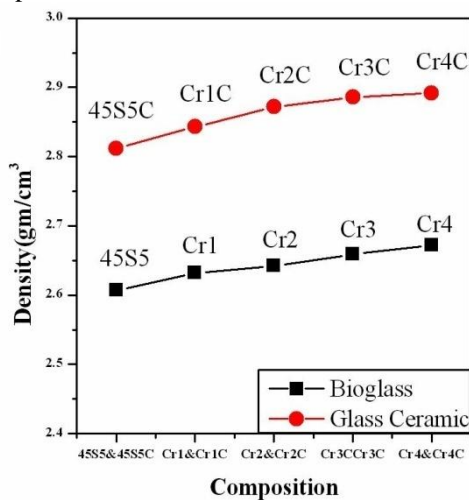


Figure.10 Density of bioglass & glass-ceramic

G. Flexural strength of bio-glasses and glass-ceramic

Fig 11 shows the results of the flexural strength for Cr0, Cr1, Cr2, Cr3 and Cr4 samples. The results demonstrate an increasing tendency in flexural strength as the percentage of chromium increases (44.48, 54.25, 61.42, 70.52 and 77.58) and glass-ceramic (104.27, 114.47, 120.20, 129.32 and 135.95 respectively).

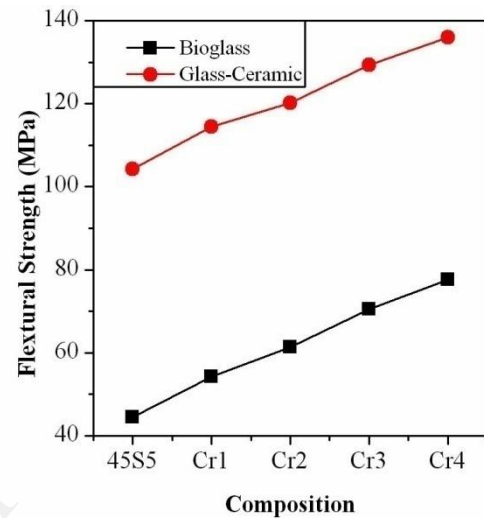
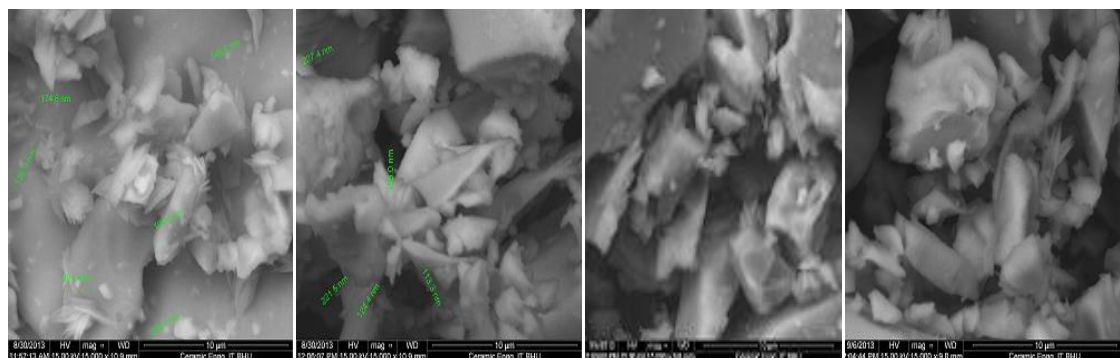


Figure.11 Flexural Strength of bioglass & glass-ceramic



(45S5)

(Cr1)

(Cr2)

(Cr3)

Figure 12. Scanning Electron Microscope (SEM) of bioactive glasses after immersion in SBF for 7 days

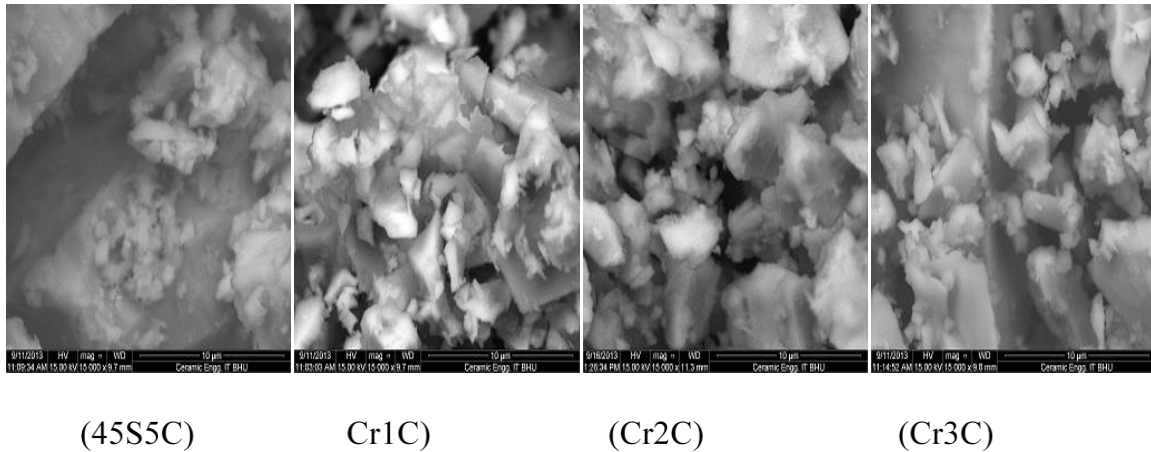


Figure.13. Scanning Electron Microscope (SEM) of bioactive glass-ceramics after immersion in SBF for 7 days

IV. CONCLUSIONS

In the present investigation, a comparative study was made on physical and bioactive properties of Cr_2O_3 substituted 45S5 bioactive glasses and glass - ceramics. The following conclusions are obtained from this investigation. The chromium substituted base bioglass showed decrease in both nucleation and crystallization temperatures. It is concluded that an increase in chromium oxide content in this series of glasses found to increase in bioactivity, this is also supported by pH and SEM analysis. Crystallized bioactive glasses decrease their bioactivity but increase their density and flexural strength compared to bioglass. The prepared bioglasses and glass-ceramics FTIR results showed the silicate network structure. The crystallized bioglasses showing main phase as $\text{Na}_2\text{Ca}_2\text{Si}_3\text{O}_9$ (Sodium calcium silicate)

REFERENCES

- [1] L. L. Hench, *J. Mater. Sci.: Mater. Med.*, 2006, 17, 967.
- [2] I. D. Xynos, A. J. Edgar, L. D. K. Buttery, L. L. Hench and J. M. Polak, *Biochem. Biophys. Res. Commun.*, 2000, 276, 461.
- [3] I. D. Xynos, A. J. Edgar, L. D. K. Buttery, L. L. Hench and J. M. Polak, *J. Biomed. Mater. Res.*, 2001, 55, 151.
- [4] R. M. Moss, D. M. Pickup, I. Ahmed, J. C. Knowles, M. E. Smith and R. J. Newport, *Adv. Funct. Mater.*, 2008, 18, 634.
- [5] S. P. Valappil, D. Ready, E. A. Abou Neel, D. M. Pickup, W. Chrzanowski, L. A. O'Dell, R. J. Newport, M. E. Smith, M. Wilson and J. C. Knowles, *Adv. Funct. Mater.*, 2008, 18, 732.
- [6] ElBatal HA, Khalil EMA, Hamdy YM (2009) *Ceram Int* 35:1195.
- [7] Hench LL, Wilson J (eds) (1993) *An introduction to bioceramics* world scientific. Singapore.
- [8] Serra J, Gonzalez P, Liste S, Chiussi S, Leon B, Perez-Amor M, Ylanan HO, Hupa M (2002) *J Mater Sci Mater Med* 13:1221.
- [9] Fatma H. ElBatal, Amany ElKhesheh, *Materials Chemistry and Physics* 110 (2008) 352–362.
- [10] Oki A, Parveen B, Hossain S, Adeniji S, Donahue H, *J Biomed Mater Res A*. 2004; 69: 216–21.
- [11] Saboori A, Sheikhi M, Moztarzadeh F, Rabiee M, Hesaraki S, Tahriri M, *Adv Appl Ceram*. 2009;108:155–61.
- [12] Balamurugan A, Rebelo AH, Lemos AF, Rocha JH, Ventura JM, Ferreira JM, *Dent Mater*. 2008;24:1374–80.
- [13] Balamurugan A, Balossier G, Kannan S, Michel J, Rebelo AH, Ferreira JM, *Acta Biomater*. 2007;3: 255–62.
- [14] M. D. O'Donnell, P. L. Candarlioglu, C. A. Miller, E. Gentleman and M. M. Stevens, *J. Mater. Chem.*, 2010, 20, 8934–8941.
- [15] Kokubo T, Takadama H, *Biomaterials* 2006; 27:2907–15.
- [16] Oana Bretcanu a, I, Xanthippi Chatzistavrou a, Konstantinos Paraskevopoulos, *Journal of the European Ceramic Society* London, 1989, p. 59.
- [17] L.L. Hench, *Journal of American Ceramic Society* 81 (1998) 1705–1728.
- [18] J. P. Nayak, S. Kumar, and J. Bera, *Journal of Non-Crystalline Solids*, 356, 1447–1451 (2010).
- [19] V.R. Mastelaro, E.D. Zanotto, N. Lequeux, R. Cortes, *J. Non-Cryst. Solids* 262 (2000) 191–199.
- [20] Rehman I, Karsh M, Hench LL, Bonfield W, *J Biomed Mater Res*. 2000 May;50(2):97-100.

**Corresponding author : Vikash Kumar Vyas
Indian Institute of Technology(BHU), Varanasi**